Design and testing of a µN - mN torsional thrust balance with wireless microwave power transmission

IEPC-2019-413

Presented at the 36th International Electric Propulsion Conference
University of Vienna • Vienna, Austria
September 15-20, 2019

K. Swar[1], D. Staab[2], A. Garbayo[3], L. Shadbolt[4]
AVS UK ltd, Oxford, Oxfordshire, OX11 0QX, United Kingdom

S. Masillo[5], A. Lucca Fabris[6], B. Karadag[7] and R. Moloney[8]
University of Surrey, Guildford, Surrey, GU2 7XH, United Kingdom

Abstract: We have designed, built and tested a new thrust balance system as an upgrade for the Electric Propulsion lab at the Surrey Space Centre (SSC). Following this proof-of-concept, our balance design will be developed as a commercial unit for other propulsion test facilities, and used in AVS' own propulsion development including microwave powered thrusters. Our torsional pendulum balance is based on flexure pivot bearings. A calibrated load cell mounted on a motorised linear stage is used for in-vacuum calibration immediately before or after thruster firing, and the displacement is measured by a high resolution optical fibre sensor. The balance includes near-zero friction electrical connections by making use of liquid metal pots centred on the pivot axis, and a wireless microwave power transfer system. Gapped waveguides are integrated into the balance to transfer up to 500 Watts of power wirelessly at 2.45 GHz while avoiding electric breakdown. The latter is key for precise characterisation of microwave-based thrusters under development at AVS. Careful consideration was given to minimising thermal drift effects and other sources of systematic errors via material selection, sensor placement and active water cooling design. Multiphysics modelling was used to optimize the wireless transmission geometry. A first test campaign in vacuum with a cold gas thruster has validated core functionality of the balance. Further tests for full performance characterisation and improvement are underway.

[1] Mechanical Engineer, kswar@a-v-s.uk.com
[2] R&D engineer, dstaab@a-v-s.uk.com
[3] Business Development Director, agarbayo@a-v-s.uk.com
[4] Project Engineer, lshadbolt@a-v-s.uk.com
[5] Ph.D Candidate, s.masillo@surrey.ac.uk
[6] Lecturer in Space Propulsion/Electric Propulsion, a.luccafabris@surrey.ac.uk
[7] Research Fellow, b.karadag@surrey.ac.uk
[8] Ph.D. Candidate, r.moloney@surrey.ac.uk

Nomenclature

θ = *Angular displacement in degrees*
τ = *Torque in Nm*
k = *Torsional spring constant in Nm/deg*
l = *Moment arm length*
F = *Force*
Δd = *Displacement*
f_n = *Fundamental Frequency*

I. Introduction

AS THE small- and nanosat market matures, increasingly capable spacecraft and challenging mission profiles are in high demand. This goes hand in hand with the development of a new generation of miniaturised, high-performance propulsion systems. Given the power, mass and volume constraints arising from nanosat platforms in particular, the vast majority of these systems produce thrust levels in the micro- to few milli-Newton (mN) range. Precision thrust balances are needed to accurately measure such low forces, which is of utmost importance during development and testing of the propulsion systems. Building these balances with sufficient accuracy and repeatability to confidently quantify propulsive performance is a non-trivial task.

Our immediate goal was to develop a new thrust balance system as an upgrade to the current experimental setup at the Electric Propulsion (EP) lab of Surrey Space Centre (SSC). This development was carried out in the framework of the UK Space Agency's National Space Technology Programme (NSTP), providing a significant boost to both SSC's and AVS capabilities in the space propulsion sector which will be valuable in future thruster development by both partners within the UK. The work was led by AVS UK in close collaboration with SSC. AVS' roadmap covering a broad range of thruster technologies also greatly benefits from this in-house thrust balance design, in particular due to its wireless power transmission capability for testing of microwave-based electric propulsion. The balance will be developed commercially in future, since the number of companies and research institutes that are in various stages of small- and nanosat propulsion development is growing dramatically and all of them require a suitable balance.

A. Requirements and target market for our Balance

1. Thrust Range

The maximum thrust range required by our primary EP market of interest is set by the thrust-to-power range of typical Hall Effect Thrusters (HETs): 60 mN/kW. To cover the market up to ~2.5 kW thrusters for larger satellite platforms, we therefore set a maximum useable range of up to 150 mN. Note this corresponds to Gridded ion engines (GIEs) up to power levels of ~4 kW. A significant fraction of the resistojet and arcjet markets up to the ~0.8 kW power level can also be covered.

The market with the largest growth potential is EP for nano- and smallsat missions. We compiled publications and datasheets for a wide variety of such thruster technologies that are already on or close to reaching the market. The corresponding thrust ranges (including small GIE & HETs, Electrospray/Colloid, Electrolysis and Electrodeless magnetic nozzle thrusters) fall between 0.01-15 mN. However the lowest thrust range of ~0.01-0.1 mN is occupied only by low-power and/or high ISP mode operations of some FEEP/electrospray thrusters, and we chose not to target this in our first balance design, preserving only the option for a future upgrade to cover this range. Nanosat cold & warm gas systems close to market are also covered by our thrust range (they fall across a wide ~0.1 – 150 mN range). Almost all chemical propulsion systems, even for the nano- and smallsat applications feature >> 150 mN of thrust; this is not the market of interest for us. Higher thrust chemical systems can exploit simpler, cheaper thrust balances than ours.

2. Maximum thruster mass and size

GIEs in the up to ~4 kW power class have masses of ~10 kg and cylindrical envelopes of order < 20 x 30 cm, while HETs in the up to ~2.5 kW class weigh < 10 kg and have envelopes of approximately < 30 x 20 x 10 cm. For the nano- and smallsat propulsion market, direct thrust measurements on fully integrated and fueled propulsion systems is often of interest during final development testing. Therefore the overall system size and wet mass should be considered, rather than just the thruster head. Based on our market survey, carried out in November 2018, the maximum system size and wet mass for nanosat systems with sufficient public data is 3U and 5 kg, although 1-2U systems with < 3 kg wet mass are by far the most common. Smallsat products can be up to 4U with wet mass of ~13 kg. Our thrust balance will allow for a total propulsion system envelope of 4U (20 x 20 x 10 cm) and 3U (10 x 10 x 30 cm). Summarizing this target market, the entire mass and size range of interest is < 13 kg and a rectangular volume of < 30 x 20 x 20 cm, which sets our requirements in Table 1.

Table 1. Top-level thrust balance requirements

Thruster mass	13 kg max.
Thruster size	30 x 20 x 20 cm max.
Thrust accuracy	5% of reading
Thrust resolution	0.01 mN in 0.1 - 1 mN range 0.1 mN in 1 - 150 mN range
Thrust range	0.1 – 150 mN

3. Thruster interfaces

At most seven DC electrical connections are required for all thrusters under consideration for testing with our balance, these should be capable of carrying up to 40 A (maximum use case for cathode heaters). Up to three separate propellant feedlines are needed for connecting to thrusters with an anode, cathode and redundant cathode. Crucially, a microwave (MW) power line capable of transmitting up to 500 Watts is needed, since AVS and SSC are developing such MW based electric propulsion systems. The frequency band of interest is ~2.2-3 GHz, but primarily at exactly 2.45 GHz.

B. State of the Art

Thrust balances in widespread use today fall under three fundamental categories of pendulum: hanging, inverted and torsional.

1. Hanging Pendulum

The main advantages of hanging pendulums are the simplicity of the design, stability and the ease of use. Such setups are relatively insensitive to problems related to the change of flexure stiffness due to heating loads during tests. On the other hand, the sensitivity of the measurements depends on a relatively long arm length, making the design more suitable for larger vacuum chamber test facilities. A hanging pendulum oscillates in the gravitational plane, making the stand response sensitive to its orientation and to the thruster mass. Compared to other designs, the standard hanging pendulum is typically the least sensitive stand type[1]. The existing balance at SSC used such a configuration.

2. Inverted Pendulum

The inverted pendulum is a high sensitivity and compact thrust stand design, although less stable than the hanging pendulum. Stability is strongly affected by the stiffness of the supporting flexures as a function of varying temperature, and active temperature control is therefore often used. In its simplest design configuration the inverted pendulum consists of a vertical arm attached to a bottom pivot and a thruster mounted at the top end. Considering the large thrust-induced deflections that the inverted pendulum can reach, study of the thruster plasma plume via fixed mounted diagnostics becomes challenging. In order to allow plasma diagnostics, parallel linkages can be implemented to mechanically block all the movements of the thrust stand except for the deflection parallel to the thrust vector. Examples of advanced inverted pendulums are the DLR's balance[2] for a thrust range up to 250mN and an accuracy of 2.5 mN and the null-type thrust stand developed at the Georgia Institute of Technology[3] with an accuracy of 2.3 mN. The inverted double-pendulum, developed by Advances Space Technologies and DLR, has two pendulum arms, connected as rigid girders to form a stiff parallelogram[2]. Two platforms are connected to the girder by flexible bearings, which allow movements only in the desired direction. The bottom platform supports the counterweight. The balance is connected to a high resolution capacitive displacement sensor and an active control system, performed with a position sensor and a voice coil. At the Georgia Institute of Technology a damper coil and a null coil has been implemented[3]. The main advantage of this null-type thrust stand design is the ability to eliminate thrust elevation effects and reduce mechanical oscillations. This stabilization is achieved with an electromagnetic actuator that counters the thrust to maintain zero relative motion of the pendulum. The thrust stand control system is based on two

PID control loops of the electromagnetic actuators: one to remove the oscillations through the damper coil and the other one for the null coil. A third PID control is used to monitor the inclination through a piezoelectric stack.

3. Torsional Pendulum

Torsional balances utilise a beam attached to flexural pivots, where a torsion spring provides a restoring force, ideally normal to the gravity vector. The rotational axis is parallel to the gravity vector, making the response of the thrust stand independent of the thruster mass. Nevertheless, gravity may affect measurements if the vertical rotational axis is offset or the centre of mass is not aligned with the rotational axis. These effects are reduced by varying the distance between the centre of mass and the spin axis, by adding a counterweight in a symmetrical arm configuration. The torsional pendulum balance has high accuracy and low environmental noise sensitivity, and can be implemented in thrust measurement ranges from µN to a few N[1]. Displacement measurements are obtained by determining the angular deflection of the beam, usually with a linear variable differential transducer or by laser triangulation systems. The sensitivity depends on the torsion spring constant, the length of the thrust stand beam and the distance of the measurement device from the axis of rotation. Compared to inverted pendulum stands, torsional stands are less compact but more stable, they are considered the pendulum type with highest sensitivity. They are susceptible to degradation of accuracy from any non-constant stiffness contribution via the thruster harness (power and propellant feed lines), so care has to be taken in the design to minimise this issue. An example of torsion-based µN thrust balance is the one developed at FOTEC[4]. The symmetrical arm torsional stand is based on a horizontal beam supported by two spring bearings and equipped with tables at both the ends, holding the thruster and a counterweight respectively. The bearing used limits the maximum load on each table to 13kg but provides a low spring rate and, therefore high sensitivity and low noise measurements with a range from few µN to several mN. Reduction of the oscillations is provided via a passive magnetic eddy current brake and deflection is measured with an optical distance transducer. Variable stiffness contribution of thruster power lines is avoided by using conductive liquid metal pots centred on the pivot axis[4].

II. Balance System Design

A. Balance Mechanism

The torsional balance acts like a moment arm being rotated as the thruster is fired. The displacement is dependent upon the torsional spring rate of the pivot point and the torque applied as

$$\theta = \frac{\tau}{k} \tag{1}$$

where θ is the angular displacement in degrees, τ is the torque in Nm, and k is the torsional spring rate in Nm/deg. The torque applied by the thruster can be calculated using

$$\tau = F \times l \tag{2}$$

where F is force in N, and l is the distance of the thrust vector from the pivot point (moment arm). The displacement Δd of the moment arm can be calculated in meters where

$$\Delta d = l \sin\theta \tag{3}$$

Equation 3 can be rearranged as

$$\Delta d = l \sin\frac{Fl}{k} \tag{4}$$

using equations 1 and 2. Using this expression, parameters such as the moment arm length l, and torsional spring rate k can be determined for varying forces. A sensitivity study was then performed using the required thrust ranges in Table 1. After investigating a range of COTS torsional flexure pivots, a flex bearing with a torsional spring rate of 5.45Nmm/deg was chosen from C-Flex Bearing Co, Inc. We selected 0.25m for the moment arm length to maximise displacement at a given thrust level, while staying within the near side sensitive range of the optical displacement sensor we have chosen. The counterweight moment arm is identical to thrust moment arm.

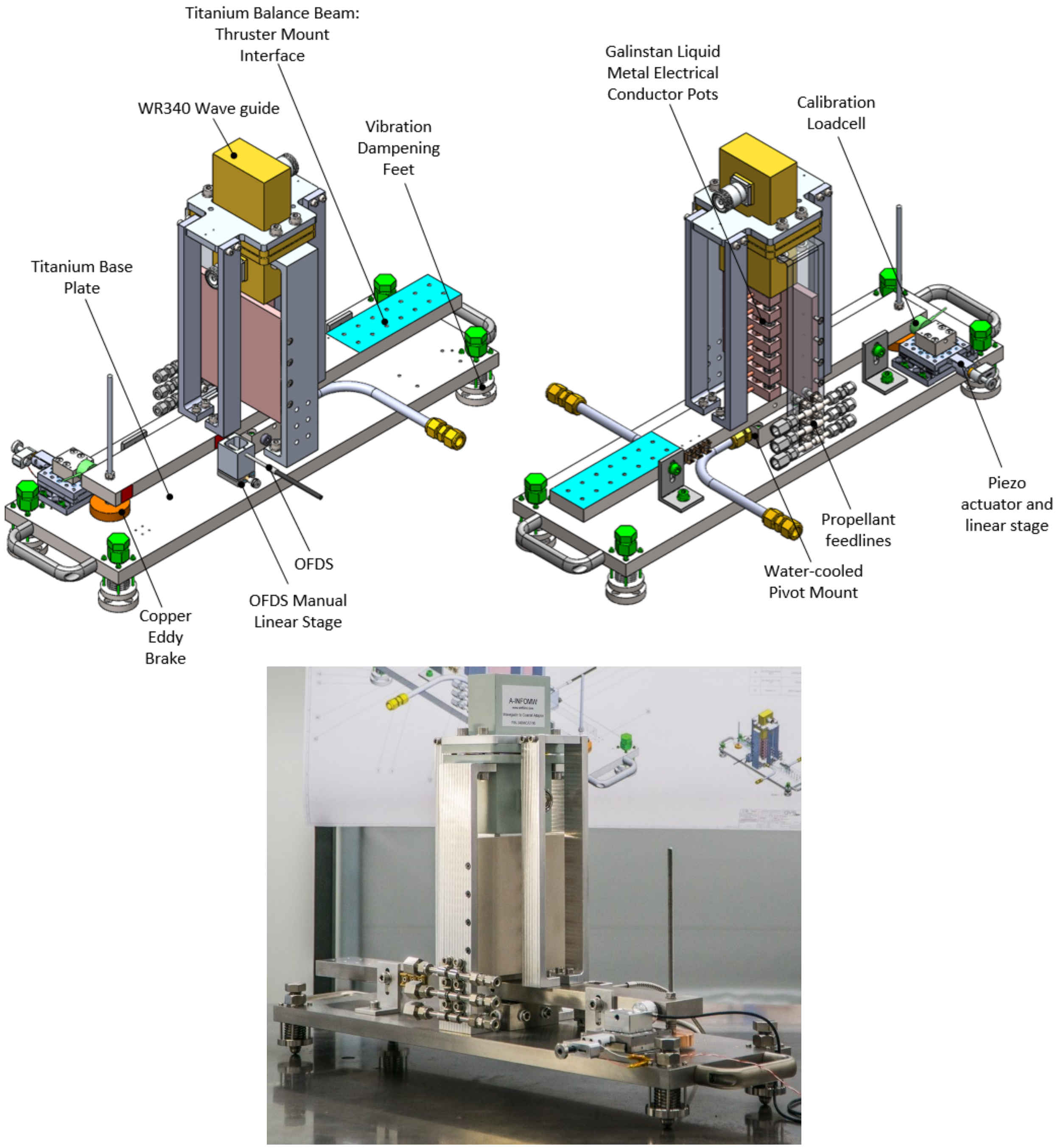

Figure 1: Thrust Balance Overview

B. Displacement Sensor

We chose to measure displacement via a COTS optical fibre displacement sensor (OFDS), as it provides very high resolution and is unaffected by electromagnetic interference induced by the thrusters likely to be tested. We selected the muDMS125 from PHILTEC with 400µm linear range on the near side, a far side range of 14.6mm, and 2.5nm resolution @ 2.5 samples/sec (its highest resolution mode). The OFDS is mounted on a manual linear stage to achieve optimum gapping for different displacements from different thrusters. The OFDS can always be kept in its most sensitive region if gapped properly, as the displacement always decreases from the gapped distance when thrust is applied. When the desired gapping is achieved for a given thruster test sequence, the manual stage can be locked and put under vacuum for thruster operation.

C. Calibration System

Historically, thrust balance calibration is often achieved by applying loads using masses of known weights on a string and pulley assembly (gravimetric method), or by non-contact forces such as an electromagnetic or electrostatic actuator. For our thrust balance, a highly sensitive load cell, F329, from Novatech was selected with 0.1N max force, and max resolution of 4μN. However, after conversations with the load cell manufacturer, the performance of the load cell was de-rated to be reliable only down to 0.1mN.

Figure 2: Novatech Load Cell with up to 0.1N force detection

The load cell is moved via a motorized linear actuator over a range of distances towards the balance arm structure, imparting a range of stepped calibration force values (nominally 9, excluding one at null position) up to the max calibration force required based on thrust range of interest. The linear stage is powered by a Newport 8302-V piezomotor with a minimum incremental value of 30nm. At each setting, the displacement will be measured by the OFDS to provide the calibration curve. This stage can be controlled remotely in the vacuum chamber so that the thrust balance can be calibrated in-situ in a repeatable manner. This method should have less uncertainty than the existing pulley system at SSC, and can be used in the very low force (thrust) regime targeted by AVS for future commercial use.

D. Damping and Levelling

We chose to add a basic spring vibration dampening system to the “feet” of the thrust balance, to attenuate vibrations caused by vacuum pumps etc. These feet are also manually adjustable via rotating M16 bolts so that the whole thrust balance can be precisely levelled and locked before vacuum operation. The levelling was done using spirit levels on both the base plate and balance beam. Vibrations with frequencies higher than the fundamental frequency of the system are dampened in a spring-mass system with dampening losses. The fundamental frequency

$$f_n = \frac{1}{2\pi}\sqrt{\frac{k}{m}} \tag{5}$$

where k is the spring rate, and m is the mass, can be used to predict the frequency at which the dampening effects begin. Without knowing the actual dampening factor, the vibration dampening amplitude cannot be accurately predicted but for our purposes, this estimation is adequate. The springs chosen were wave-springs by Smalley as standard helical coil springs would take up too much vertical space. As there are four points of contact on the thrust balance base plate, four spring rates were added together to form a total spring rate k. The mass of the system (thrust balance, high mass thruster and counter-weights) was estimated using worst-case assumptions. From this, the displacement of the springs due to the mass of the system can be calculated using

$$x = \frac{F}{k} \tag{6}$$

where F is the force due to mass, and k is the spring rate. A CM28-H9 spring from Smalley was chosen to satisfy the worst case displacement due to mass of the system, with as low of a fundamental frequency as possible. The worst case loading allows for a fundamental frequency of 4.88Hz and a 1kg thruster allows for a fundamental frequency of 6.93Hz. Both of these values are below the observed environmental vibration conditions found at Imperial College London’s vacuum chamber facilities[5], so similar vibration environment at SSC should be adequately damped by the springs.

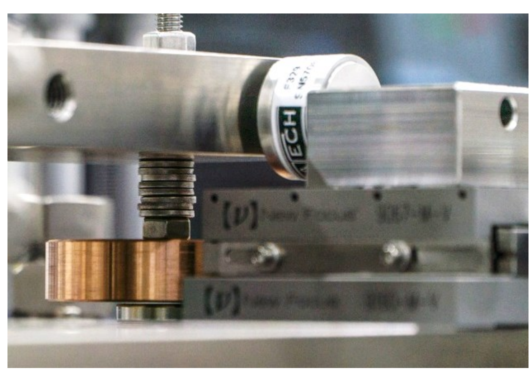

Figure 3: Side view of thrust balance with copper eddy brake system installed.

In addition to reducing vibrations from the vacuum chamber and facility, we added a passive eddy brake system to dampen the oscillations due to the initial pulse of thrust as shown in Figure 3. A Ø50mm copper disk with 12.7mm thickness was used in conjunction with two N35 magnets with Ø22 and 4mm thickness stacked on top of each other. The bottom magnet was epoxied onto the base plate.

E. Thermal Design

Low thermal expansion and high thermal conductivity materials were preferred to reduce thermal drift effects. Non-ferromagnetic metals also have to be used to avoid magnetic interactions with thrusters using powerful permanent or electromagnets, in addition to minimising the use of stainless steel (which shows magnetism to varying degree for some grades after manufacturing processes). Typical composite materials on the other hand would lead to outgassing problems in vacuum. The preferred material we used throughout our balance, in particular for components that would likely affect thermal drift, is Titanium (note the lower thermal expansion coefficient and high enough thermal conductivity, compared to Aluminium).

The bearing hub which houses the flexure bearing has a U-shaped internal channel wrapping around the bearing seat. This allows for water cooling to reduce thermal drift and change in torsional stiffness of the bearing during thruster operation. The water supply is from a Wilkinson Star WRC-300 water cooler with a flow rate of 8.5L/min at around 1.5-2bar and 15-20C.

F. Electrical Connections

Electrical connections needed for thruster operation introduce undesired stiffness elements to the thrust balance system that can vary with temperature, reducing repeatability of the balance measurements. To eliminate this problem, liquid metal connections were implemented in our design. Galinstan (a commercial name for a liquid metal alloy consisting of mainly Gallium, Indium, and Tin) was used, as it is a liquid metal at room temperature and has a very favourable vapour point for use in vacuum environments. It is also non-toxic (unlike mercury) and has been successfully demonstrated in the thrust balance literature.

Non-conductive PEEK pots were used to contain the Galinstan. Copper rods were used for electrical connections. The "input" copper rods are dipped in the Galinstan pots and remain stationary while the pots themselves rotate as the balance beam displaces due to thrust. This rotation is in line with the pivot axis so no additional friction is incurred. This allows for an almost frictionless electrical connection, as there will still be some minimal unavoidable friction from the viscosity and surface tension of Galinstan.

Figure 4: Electrical connections using RT liquid metal Galinstan

G. Propellant Feedlines

A simple feedline hub for propellant was designed with ¼'' tubing input and ¼'' NPT output for robustness. This hub function as a stationary and repeatable fixing point for flexible propellant feedlines as it is not affected by changes in thruster mounting. A tubing holder on the balance beam also fixates the flexible tubing, making it another stationary and repeatable fixing point on the rotating beam. The propellant feedlines between their 2 fixed locations on the hub and balance beam, and thermocouples are the only significant stiffness contribution to the thrust balance apart from the flexure pivot. In practice however, we found that the PTFE tubing contributed more stiffness than expected which moved the null-position, which is the position of the balance beam without thrust applied, from its nominal point. A redesign of the propellant feedline hub is therefore underway to mitigate this issue.

H. Wireless Microwave Power Feed

Two rectangular waveguide sections are used to transfer wireless MW power at the interface from the stationary balance side to the rotating balance beam side, instead of coaxial cables attached directly to the thruster. This eliminates the large and temperature-variable stiffness contribution of coaxial cables carrying up to 500 Watts of power. Given the overall torsional balance design and requirements, such a wireless system is unavoidable. The support structure for the two WR340 waveguides is manufactured from Aluminium. They are rated for 2.2-3.3 GHz, up to 500 Watts, and include 7/16'' DIN female coaxial connectors. The transmitting waveguide, connected via cables to a microwave generator, is fixed to the base plate and will remain stationary. The receiving waveguide, connected to the thruster via a short coaxial cable, will be fixed to the balance beam and will rotate with it. There is a 1mm contactless gap between the two waveguides, and none of the cables exerts a force on the balance as they both remain stationary with respect to their mounting points. Combined with electrical isolation via ceramic washers in the thruster interface plate and the waveguide mounting structure, this gap also effectively blocks transmission of any DC current through the MW line. This is vital for the operation of MW-powered cathodeless ambipolar thrusters[6 7], and eliminates the need for a separate DC block component which would cause non-negligible power dissipation and losses on the line.

Since the 1mm gap between waveguides is far smaller than the microwave wavelength at 2.45 GHz, it is expected to cause small transmission losses. We quantified this via multiphysics software, modelling the exact waveguide interface geometry of our design, and performing an S-parameter calculation. This was repeated for a series of gap widths - as shown in Figure 5, the power loss scales linearly with gap width and at 1mm, 98.9% of input power is transmitted across the gap. Note that we ruled out widths below 1mm, as a combination manufacturing tolerances and low-level thermal expansion of the waveguides during operations could cause the gap width to become unacceptably small: <0.5mm, where electric breakdown risks arise (see below). Using the same model, we verified that the transmission losses remain unaffected by the maximum rotation of 0.1 degrees between the waveguides that will occur for our balance design at the highest thrust and deflections levels. Similarly, lateral in-plane misalignments between the waveguides of up to 3 mm were found to have a completely negligible effect on the transmission loss, with 98.7% of power transmitted in the worst case.

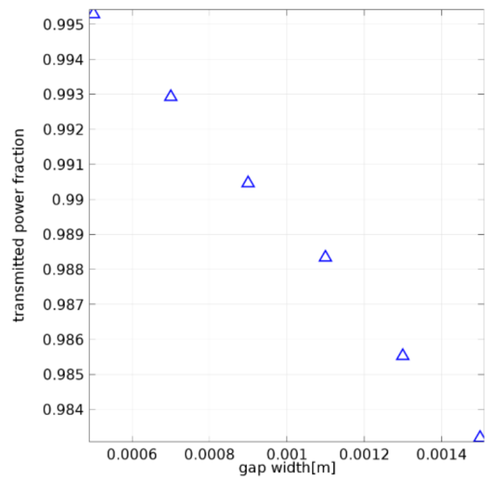

Figure 5: Predicted power transmitted across the two waveguides as a function of gap width.

As the wireless interface is a custom design with localised high electric field strengths, we assessed the potential for electric breakdown to occur in this region in the relevant vacuum conditions. Such breakdown could cause localised plasma production at high input power levels with uncertain effects on the balance's repeatability, and in the worst case component failure. During standard operations of electric propulsion systems, the vacuum chamber background pressure will always be $<10^{-3}$ Torr, which is the threshold for multipactor MW breakdown effects. In this regime, breakdown is pressure independent and it can occur if a critical voltage between small gaps is exceeded. We followed ECSS-E-20-01A methodology[8] and thresholds for multipactor breakdown calculation. This document tabulates the breakdown voltage for gaps between aluminium surfaces (as for our waveguides), as a function of the fD parameter, the microwave frequency f multiplied by gap width D. For our case, fD = 2.45 GHz mm, and the breakdown voltage is 100 V exactly. Using the same multiphysics model as for the power loss calculation, we found the maximum voltage across the waveguide gap in our design is 49V, at 500 Watts of input power. At our maximum design power we are therefore a factor of 2 below the critical breakdown voltage. Note that this voltage scales with the square root of input power.

III. Preliminary Tests

A. Experimental Setup

All tests were performed in the Pegasus vacuum chamber at the electric propulsion laboratory of SSC. The torsional thrust balance was placed on a stand attached to the inside of the door of the vacuum chamber for both ambient and vacuum calibration and cold gas thruster testing. The Pegasus chamber has a length and internal diameter of 1.2m and is equipped with the relevant feedthrough ports for interfaces with the balance's propellant lines and sensor signal lines. Pressure gauges are installed at locations of interest in the vacuum system and are used to monitor pressure in the chamber and lines. During operation with the thrust balance, only the roughing pump was activated, reaching background pressure of order of 8 mbar which is sufficient for our cold gas tests. Our primary goal in these initial tests was to verify the core functionality of the balance, including in-vacuum calibration, and gather first thrust data using a very simple thruster.

Calibration was carried out with the thruster mounted on the balance in the exact configuration as during firings, so that the stiffness of the gas feed lines was fully accounted for when evaluating the equivalent stiffness of the system. The propellant lines were assembled in such a way to minimise interferences or variable friction on the balance beam. To mitigate thrust measurement errors related to an unwanted inclination of the vertical rotation axis or an offset of the centre of mass with the rotational vector, the levelling procedure and checks with a spirit level were carried out immediately before calibration or thrust measurement, and correct counterweighting was implemented throughout. For this cold gas thruster testing campaign, counterweights with combined mass of 890g were used to balance the weight of interface plate and cold gas thruster.

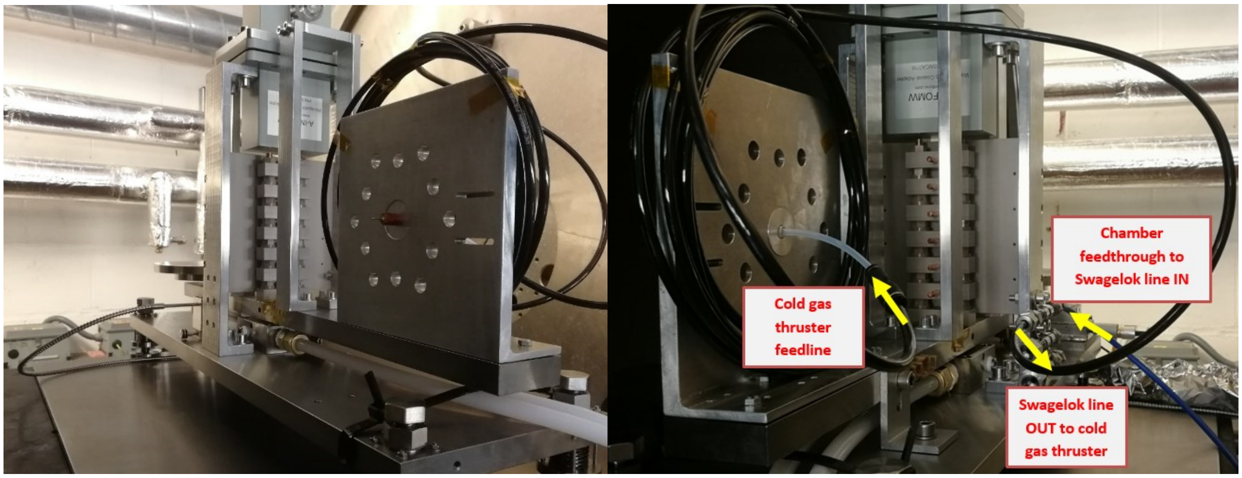

Figure 6: Experimental Test Setup

1. Cold gas system

Two different cold gas thrusters were used to cover a range of thrust magnitude at the ~ 1-10 mN level. These 2 cold gas systems have near-identical designs, based on a pre-assembled one-piece COTS orifice attached in the same way to the propellant feedlines and interface plate, ensuring a repeatable setup. Their minimum orifice internal diameters (throat sizes) were 0.10 mm and 0.25 mm respectively. Three different levels of thrust for each system were achieved by setting the upstream pressure level to 1, 2, and 3 bar. This was achieved via manual regulation of a valve installed on the propellant tank equipped with an analog display. The propellant used throughout this testing campaign was Argon. The thrusters were fired for ~50 seconds before closing the upstream valve. For each thrust level, 3 measurements were taken to quantify the repeatability of the system. The thrust was calculated as the mean of the three measures and the uncertainty as 3σ. Note that while these cold gas thrusters had not previously been characterised on a different balance, we predicted their thrust levels using basic isentropic flow calculations to range from 0.8 to 8 mN at these upstream pressures. Lower and higher thrust levels, covering the full range of our Balance (c.f. Table 1) will be covered in future test campaigns.

2. Calibration

The calibration followed the basic procedure outlined in Section C. The calibration procedure involved the application of 9 calibration force values, equally spaced between 0.6 and 6 mN. Those calibration force values were applied and recorded via the loadcell, moved via the motorised linear actuator and linear stage. The OFDS measured the displacement of the balance beam at each force increment, applied for 30 seconds. The raw load and displacement timeseries were smoothed by using a 5^{th} order Butterworth filter with cut-off frequency of 0.5Hz. Then the calibration factor k was computed as linear interpolation of the data of the balance displacement increments measured by the OFDS and the load increments read with the load cell. The entire calibration procedure was repeated 5 times both in ambient conditions and in vacuum, yielding a set of calibration factors k, to assess repeatability. The uncertainty of k was measured as 3σ, where σ is the standard deviation over the 5 calibrations.

B. Experimental Results

1. Calibration

The damping system of the thrust balance was tested before starting the calibration. The applied force referred to the highest reachable thrust magnitude of the testing campaign. The damping system consists of a copper disk and permanent magnet whose position could be changed by adding/removing washers on the M6 threated rod that holds the permanent magnet. A number of 10 washers was enough to obtain an underdamped response of the system as can be observed in Figure 7 which is a displacement over time plot of the OFDS raw data. This plot refers a thrust level of about 8mN.

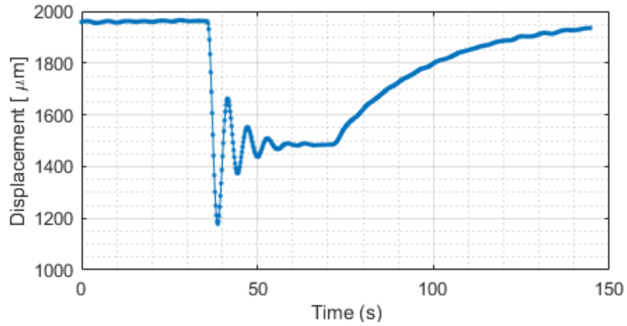

Figure 7: Test on the damping system of the thrust balance, underdamped response to 8mN force.

An example of the calibration raw and filtered data for both load cell and OFDS in vacuum conditions are shown in Figure 8.

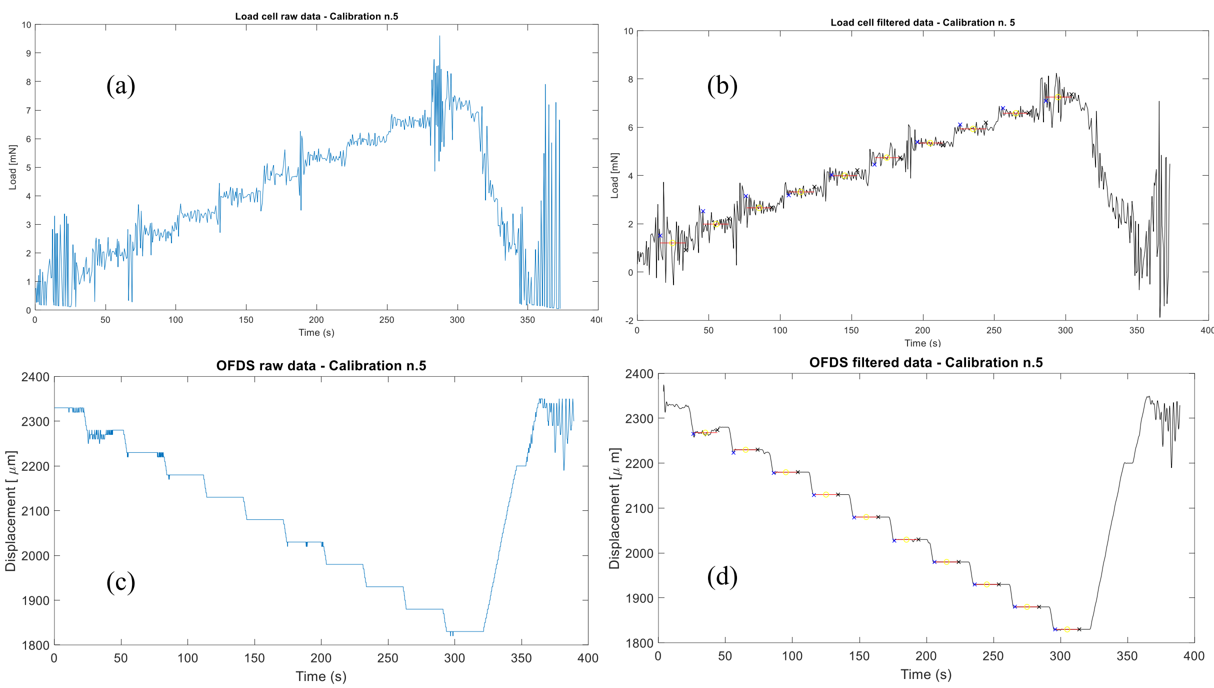

Figure 8: (a) Raw load cell calibration steps. (b) Filtered load cell calibration steps. (c) Raw OFDS calibration steps (d) Filtered OFDS calibration steps.

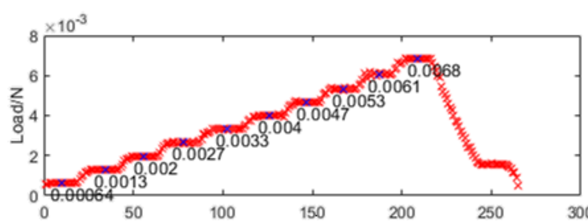

Figure 9: Load cell performance during calibration runs before final integration demonstrating normal noise behaviour.

Figure 8 (a) shows the noise present in the load cell raw data and it is unexpectedly noisy compared to earlier tests performed before full integration as shown in Figure 9. We have ruled out vibrations from the immediate vacuum chamber turbo-pumps as similar noise was present in both ambient and vacuum conditions although both tests were performed in a vacuum chamber facility with other noise sources. Electrical noise was also minimised by the use of shielded twisted pair cables. We have also ruled out any kind of micro vibrations that is not parallel with the force vector by pushing the load-cell onto the balance beam in its locked state. In any case, the noise observed is unusual and must be electrical or internal to the load cell as the OFDS does not display the same noise behavior if the noise were to be mechanical. By interpolating the mean load cell and mean OFDS data, the calibration curve was computed as shown in Figure 10. The linearity of the fitting curve was demonstrated, the calibration factor k and the uncertainty of the calibration factor was calculated to be 0.020+/-0.00116N/mm. The calibration factor in ambient conditions was also calculated to be 0.013+/-0.00026N/mm.

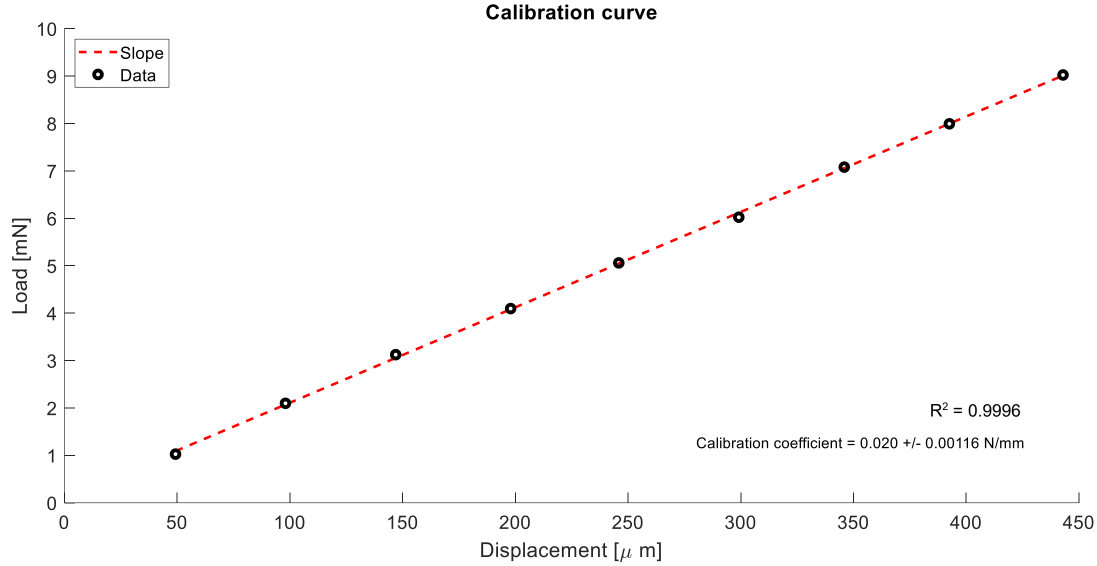

Figure 10: Calibration curve evaluated in vacuum condition

2. Cold gas thrust

When the cold gas thruster was activated, the displacement data before and after the detected step point were computed and interpolated with the calibration factor to obtain the thrust. Example of the recorded filtered data of the Argon propellant orifice with 0.25mm nozzle diameter and upstream pressure of 3bar are shown in Figure 11. The null and steady-state position ranges were selected and averaged to further eliminate noise. Note that the trailing edge showing the slow decay of thrust displacement is due to the propellant slowly escaping from the long length of tubing used between the orifice and flow valve. The sensor of the vacuum chamber registered a pressure of 8.33mbar. The full array of test results for 2 nozzle sizes at 3 upstream flow pressures is shown in Figure 12.

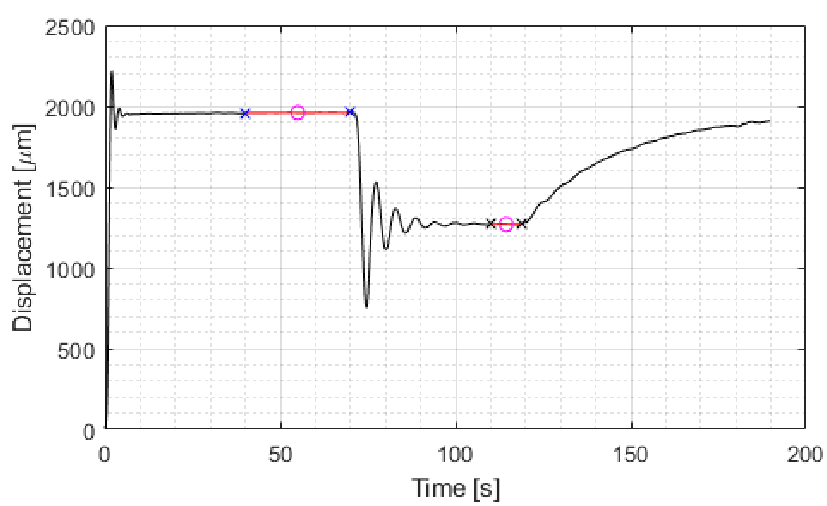

Figure 11: An example plot of filtered OFDS thrust balance displacement data, with selected null and steady state positions. Vacuum chamber at 8.33mbar, cold gas thruster with 0.25mm nozzle diameter and upstream pressure at 3bar, Argon. Displacement corresponds to around 9mN of thrust.

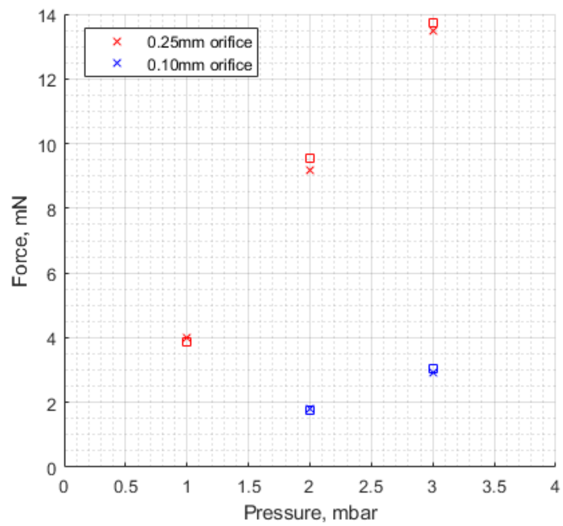

Figure 12: Thrust magnitudes of 2 cold gas systems with different orifice sizes working at 3 upstream pressures. Square and cross marks denote each repetition at the same pressures.

The sources of uncertainty on calibration factor certainly arise from the significant noise of the load cell data during calibration. There is a remarkable difference in uncertainty between ambient and vacuum calibration factors which means this can be addressed by reducing the vibrations of the thrust balance in vacuum. The quality of data recorded at this time with the cold gas orifices could be improved as we are still refining the operation and knowledge of the instrument. Due to this we could only supply indicative repeatability of the thrust balance as shown in Figure 12.

IV. Conclusion

A torsional thrust balance was designed, built, and tested in ambient and vacuum conditions with multiple cold gas thruster orifices. Thrust measurements from 1.79 to 13.6mN were recorded. Thrust response was underdamped through a magnetic damping system although the response can be modified to critical damping in future tests for faster response times. Further improvements and operational refinements will be pursued to improve the noise performance. More thruster systems will be tested including the wireless microwave power feed.

Acknowledgments

The work described in this paper is funded by the UK Space Agency's National Space Technology Programme in the framework of the "NSTP3-PF2-055" project. K. Swar would like to thank technicians at AVS for assistance during integration. The authors would also express their gratitude to the vacuum test facility staff at Surrey Space Centre for technical assistance during test integration and test campaign.

References

[1] Polk, James E., et al. Recommended practices in thrust measurements. No. IEPC-2013-440. CALIFORNIA INST OF TECHNOLOGY PASADENA JET PROPULSION LAB, 2013.
[2] Neumann, Andreas, Julian Sinske, and Hans-Peter Harmann. "The 250mN Thrust Balance for the DLR Goettingen EP Test Facility." 34nd International Electric Propulsion Conference, IEPC-2013. Vol. 211. 2013.
[3] Xu, Kunning G., and Mitchell LR Walker. "High-power, null-type, inverted pendulum thrust stand." Review of Scientific Instruments 80.5 (2009): 055103.
[4] Seifert, B., et al. "Development and verification of a μN thrust balance for high voltage electric propulsion systems." 33rd International Electric Propulsion Conference, Washington, DC. 2013.
[5] Liu, G., Knoll, A., "Development and Testing a Novel Millinewton Thrust Balance for Plasma Thruster Performance Characterization", MSc Dissertation, Imperial College London, 2018, (unpublished)
[6] Rosati Azevedo, E., et al., "Analytical Plasma Modelling and Design Upgrade for an ECR Thruster Operating on Water and Ammonia Propellants," *Proceedings of the 36th International Electric Propulsion Conference*, CP638, Vienna, Austria, 2019, (to be published)
[7] Moloney, R., Karadag, B., Lucca Fabris, A., Staab, D., Frey, A., Garbayo, A., Shadbolt, L., Rosati Azevedo, E., Faircloth,D., Lawrie, S., and Tarvainen, O., "Experimental Validation and Performance Measurements of an ECR Thruster Operatingon Multiple Propellants,"The 36th International Electric Propulsion Conference, Vienna, 2019
[8] Design, Multipaction, and E. C. S. S. Test. "Secretariat: ECSS-E-20-01A." ESA-ESTEC May 5 (2003)